Estimation of the Rebar Force in RC Members from the Analysis of the Crack Mouth Opening Displacement Based on Fracture Mechanics

Pengru Deng, Takashi Matsumoto

Journal of Advanced Concrete Technology, volume 15 (2017), pp. 81-93

Scientific paper

Estimation of the Rebar Force in RC Members from the Analysis of the Crack Mouth Opening Displacement Based on Fracture Mechanics

Pengru Deng[1] and Takashi Matsumoto[2*]

Received 4 November 2016, accepted 8 February 2017 doi:10.3151/jact.15.81

Abstract

A method for estimating the rebar force crossing a crack under model I loading in RC beams using the crack mouth opening displacement (CMOD) is proposed based on fracture mechanics accounting for bond slip at rebar-concrete interface. In the method, a CMOD is regarded as a consequence of the combined action of applied loads, rebar bridging forces and the bond slip. The CMOD due to these three contributors are estimated through an integral transformation based on fracture mechanics and a bond slip model. Since the CMOD due to bond slip is included, the tension stiffness effect is considered implicitly. Theoretically, the rebar force is estimated through the proposed method and the inverse analysis of COD profile using the same noisy synthetic COD profile. The smaller error of the proposed method in most cases demonstrates its reliability. The proposed method is further investigated through estimating the rebar force of an RC beam subjected to four-point bending load in laboratory, where acceptable accuracy is achieved. Conclusively, as the proposed method is dedicated to rebar force estimation of an RC member using CMOD, it provides a potential NDT&E approach for existing structures where the COD profile cannot be measured.

1. Introduction

In reinforced concrete (RC) structures, by incorporating ductile steel rebars into brittle concrete matrix allows to improve several mechanical properties, such as cracking resistance, ductility, impact resistance and fatigue resistance. Therefore, stress level in the rebars is an important indicator of the structural performance, and rebar force estimation plays an important role in structural health monitoring (SHM) and maintenance of RC structures. Unfortunately, the rebar force cannot be measured directly in existing structures, unless embedded sensors have been installed during construction. Nevertheless, the rebar force that is responsible for crack bridging has inherent connection with structural surface cracks. This connection provides a possibility of estimating rebar force through an indirect approach.

Generally, in concrete structures, the effect of crack bridging forces due to a variety of elements (rebars, aggregates and fibers) is effectively modelled by a continuous distribution of stresses acting on crack faces. The integral transformation relating crack opening displacements (COD profile) with crack opening stresses due to applied loads and crack bridging forces for various geometries and load conditions have been proposed in (Cox and Marshall 1991; Fett *et al*. 1996; Marshall *et al*. 1985; Marshall and Cox 1987; McMeeking and Evans 1990) based on fracture mechanics. Inversely, the estimation of crack bridging forces acting on the crack faces using the measured COD profile has been successfully applied in (Buchanan *et al*. 1997; Cox and Marshall 1991). By assuming rebar forces as a step function and following a weight function method for determining the stress intensity factor (SIF), a transformation between the rebar force crossing a crack under model I loading and the COD profile has been derived in Nazmul and Matsumoto 2003. This transformation has been applied successfully in estimating the rebar force in cracked RC beams under four-point bending load through inverse analysis of the experimental COD profile in (Nazmul and Matsumoto 2008a, 2008b), where Tikhonov regularization method and linear filter method were employed in addressing the ill-posed problem and the randomness due to noisy COD data, respectively. However, for many concrete structures, such as slabs, the COD profile is difficult to be measured, or it is even unmeasurable. Also complicated mathematical methods are necessary in addressing the noise in measurement data. Therefore, a convenient, reliable and sophisticated technique using easily accessible data deserves great attention in infrastructure maintenance.

In this paper, an estimation method of rebar forces crossing a crack under Model I loading conditions in RC structures is proposed through using only the crack mouth opening displacement (CMOD) based on fracture mechanics and local bond slip model. As a result, the complicated process of measuring and optimizing COD profiles is obviated. Thus, this method is a potential non-destructive test and evaluation method for RC members where the COD profile is difficult to be measured. In addition, this method is superior to some other simpler rebar force estimation methods, e.g. sectional analysis method, because the contribution of bond slip

[1]Graduate School of Engineering, Hokkaido University, Hokkaido, Japan.
[2]Professor, Faculty of Engineering, Hokkaido University, Hokkaido, Japan. *Corresponding author,
E-mail: takashim@eng.hokudai.ac.jp

in the rebar-concrete interface on the CMOD is considered through employing a bond slip model. As a result, the corresponding influence of bond slip on the rebar force, which is known as the tension stiffness effect, can be captured. Since this method is dedicated to providing a potential non-destructive test and evaluation approach of existing RC members, no crack propagation maybe assumed in all computations.

2. Problem formulation

Consider a crack in an RC structure under external load, the crack opening is governed by two mechanisms: the activation of bond forces at the rebar-concrete interface and the bridging effect of rebars crossing the crack. Over the last few decades, both mechanisms have been extensively studied in different fields and through different approaches (Ben Romdhane and Ulm 2002; Eligehausen *et al*. 1982; Harajli *et al*. 2002; Li and Liang 1986; Li and Matsumoto 1998; Okamura *et al*. 1985; Salem and Maekawa 2004).

To better understand the concrete crack opening process, this process is interpreted as consisting of two steps. Step 1: Perfect bond is assumed. The crack opens under applied loads and rebar bridging forces. The resulting crack profile is shown in **Fig. 1** marked as Line 1. Step 2: Bond slip occurs at rebar location and then transfers to the other positions along the crack. Correspondingly, the COD profile shifts to Line 2 in **Fig. 1**. In Step 2, the rebar bridging force changes as a consequence of the shift due to bond slip. In previous studies dealing with the inverse analysis of COD profiles, the crack bridging force along the crack can be estimated without considering bond slip because the COD profile shift due to bond slip can be captured and then reflected on the basis of the change of the crack bridging force estimated through inverse analysis. Therefore, the actual bond slip is implicitly included and the result of inverse analysis of COD profile is the bridging force distribution along the crack regardless of where the bridging force comes from. On the contrary, the COD utilized in this study is only CMOD, which means that only the change of COD due to bond slip at crack mouth can be captured, while the bond slip has a more significant contribution to the COD profile shift at the region close to rebar. This local COD profile shift is a manifestation of the popular tension stiffening effect of concrete which reflects the ability of concrete to tension between cracks. Due to the existence of tension stiffening effect, the rebar force decrease by a certain extent according to the bond strength between concrete and reabrs. Thus, rebar force estimation of existing RC members cannot be successfully conduced if the tension stiffening effect is not considered appropriately.

Therefore, this study establishes the rebar force estimation method by calculating the bond slip related CMOD separately through introducing local bond slip model and then eliminates it from the experimental CMOD. The remaining CMOD due to rebar bridging forces and applied loads is calculated based on fracture mechanics by using the weight function method in determining the stress intensity factor. Since the method is based on the general cracking mechanisms of RC structures, theoretically, this method can be applied for force estimation of rebars crossing cracks if the corresponding weight function and bond slip model are available. To verify the applicability of this method, this study is focused on relative simple crack problems, i.e. the cracking problems of RC beams under Mode I load conditions, which can be achieved by a RC beam with a crack at the midspan under pure flexure as shown in **Fig. 1**. According to the method used for the calculation, the CMOD is divided into two: CMOD due to applied loads and rebars and CMOD due to bond slip, which will be introduced separately.

2.1 CMOD due to applied load and rebar bridging forces

For the crack geometry shown in **Fig. 1**, such a single dominate crack at the midspan resembles a single edge notch (SEN) fracture specimen, and a zero or negligible shear at the crack plane ensures Mode I fracture. A two-dimensional bridged crack model is exploited for the through-the-thickness cracked RC beam. Therefore, the

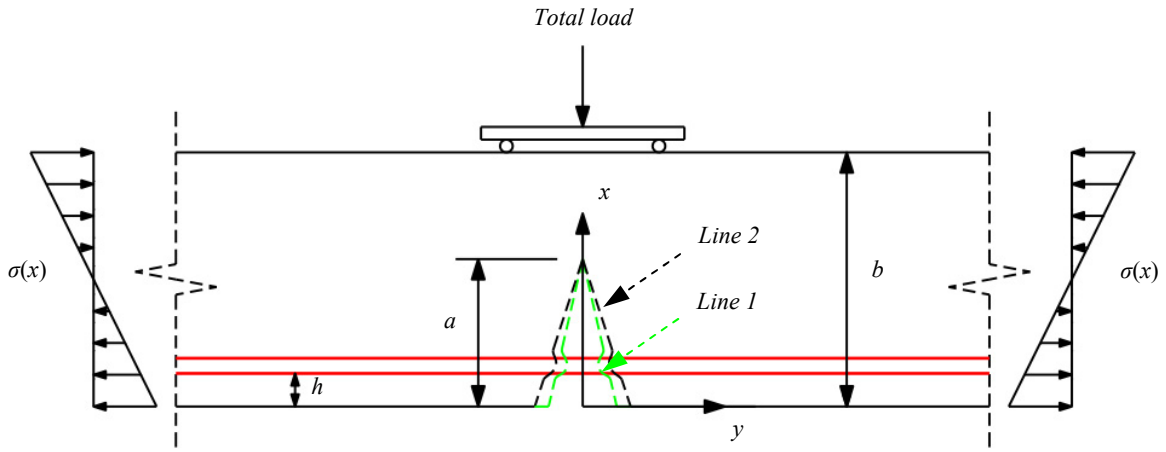

Fig. 1 Schematic diagram for the understanding of cracking process.

relevant quantities are applicable to unit thickness of the beam.

Linear elastic behavior of rebar and concrete is assumed after the crack has passed the rebars. Since this method is dedicated to the non-destructive test and evaluation of a cracked RC member, no crack propagation is assumed. Correspondingly, the nonlinear effect due to the fracture process zone is out of the research scope. Therefore, the CMOD due to applied loads and rebar bridging forces is calculated following the integral transformation for a bridged crack in an elastic medium (Cox and Marshall 1991) based on fracture mechanics. Consider an existing crack in a RC beam, in order to calculate the COD at any location along the crack, a virtual line load P is applied at that location. Following Castigliano's theorem (Sokolnikoff and Specht 1956), the displacement at that position is given by

$$u(x) = \lim_{P\to 0} \frac{\partial W}{\partial P} \tag{1}$$

where x is the distance between the target position and the bottom face of the beam as shown in **Fig. 1**. W is the total strain energy of the system per unit width of crack front. Thus the derivation is valid only if the system is linear-elastic, apart from the nonlinearity in the action of crack bridging stress. The strain energy may be written as an integral of the strain energy release rate per width of crack front, which is denoted as $\mathcal{G}$

$$W = \int_0^a \mathrm{G} da' = \int_0^a \frac{K_{tip}^2}{E'} da' \tag{2}$$

where a is the crack length which can be identified following the procedure described in (Nazmul and Matsumoto 2008a), a' is the dummy variable for a. E' is a combination of elastic constants, which depends on whether the problem is in plane stress or plane strain conditions and also on whether the material is isotropic or orthotropic. For isotropic materials

$$E' = \begin{cases} E_c & \text{for plane stress} \\ \dfrac{E_c}{1-\nu^2} & \text{for plane strain} \end{cases} \tag{3}$$

where v is Posson's ratio of concrete, E_c is the Young's modulus of concrete, K_{tip} is the superposed effect of applied loads, bridging forces and the virtual load P.

$$K_{tip} = K_a + K_b + K_P \tag{4}$$

where K_a and K_b are SIF owing to applied loads and bridging forces, respectively. K_P is SIF due to the virtual load P.

To facilitate the derivation of a transformation between bridging force and COD, the stress intensity factors are determined according to the weight function method proposed by (Bueckner 1970; Rice 1972) because once the weight function for a particular crack is determined, the stress intensity factor for any loading system can be calculated. Based on the weight function method, the SIF due to the virtual load P is

$$K_P = \begin{cases} G \cdot P & x < a \\ 0 & x \geq a \end{cases} \tag{5}$$

where G is a weight function which depends on the crack geometry only. The weight functions for a variety of significant geometries can be found in handbooks for crack analysis [e.g. (Tada *et al*. 2000)]. For the SEN specimen under Mode I load conditions, the weight function is given as

$$G(x,a,b) = \frac{1}{\sqrt{\pi a}} \frac{h_1(x/a, a/b)}{\left(1 - x^2/a^2\right)^{1/2}} \tag{6}$$

where b is the beam depth, and

$$h_1(x/a, a/b) = \frac{g(x/a, a/b)}{(1 - a/b)^{3/2}} \tag{7}$$

assuming $a/b=\xi$, then

$$g(x/a, a/b) = g(x/a, \xi) \tag{8}$$

and

$$g(x/a, \xi) = g_1(\xi) + \frac{x}{a} g_2(\xi) + \frac{x^2}{a^2} g_3(\xi) + \frac{x^3}{a^3} g_4(\xi) \tag{9a}$$

$$g_1(\xi) = 0.46 + 3.06\xi + 0.84(1-\xi)^5 + 0.66\xi^2(1-\xi)^2 \tag{9b}$$

$$g_2(\xi) = -3.52\xi^2 \tag{9c}$$

$$g_3(\xi) = 6.17 - 28.22\xi + 34.54\xi^2 - 14.39\xi^3 - (1-\xi)^{3/2} - 5.88(1-\xi)^5 - 2.64\xi^2(1-\xi)^2 \tag{9d}$$

$$g_4(\xi) = -6.63 + 25.16\xi - 31.04\xi^2 + 14.41\xi^3 + 2(1-\xi)^{3/2} + 5.04(1-\xi)^5 + 1.98\xi^2(1-\xi)^2 \tag{9e}$$

Substituting Eqs. 5 and 6 into Eq. 1, the following equation is derived.

$$u(x) = \frac{2}{E'} \int_x^a (K_a + K_b) G(x, a', b)\, da' \tag{10}$$

Furthermore, K_a and K_b can be also computed through weight function method. Considering stresses are acting on two opposite faces of the crack, then

$$u(x) = \frac{4}{E'} \int_x^a \left[\int_0^{x'} G(x', a', b)\left[\sigma(x') - f(x')\right] dx' \right] G(x, a', b)\, da' \tag{11}$$

where $\sigma(x)$ is the stress that would exist on the crack faces in the absence of a crack and $f(x)$ is the stress on crack faces due to rebar force per unit length along the crack. x' is the dummy variable of x. Correspondingly, defining $u_a(x)$ and $u_b(x)$ as the crack opening and crack closing due to applied load and rebar bridging, separately, then the complete forms of these two components of COD are

$$u_a(x)=\frac{4}{E'}\int_x^a\left[\int_0^{a'}G(x',a',b)\sigma(x')dx'\right]G(x,a',b)da' \quad (12)$$

$$u_b(x)=-\frac{4}{E'}\int_x^a\left[\int_0^{a'}G(x',a',b)f(x')dx'\right]G(x,a',b)da' \quad (13)$$

For the cracked RC beam under pure bending loads as shown in **Fig. 1**, linearly distributed bending stresses would exist on the crack face in the absence of the crack according to the widely-approved plane cross-section assumption for a linear elastic system. Thus, the stress distribution due to applied load should be:

$$\sigma(x)=\sigma\left(1-\frac{2x}{b}\right) \quad (14)$$

where σ is the maximum stress at the extreme concrete fibers.

The linear elastic behavior is assumed until rebar yielding. The post-yielding behaviors do not need to be considered because the focus of this study is existing structures under service loads.

The term $f(x)$ is assumed as a step function following (Nazmul and Matsumoto 2008a).

$$F=\frac{M}{jd} \quad (15)$$

$$f(x)=f\cdot\left[H(x-h)-H(x-h-d_b)\right] \quad (16)$$

where M is the acting bending moment, jd is the internal lever arm between the tension force of rebars and the resultant compression force of concrete, where d is the effective beam depth. h and d_b are clear distance of rebar from the bottom face and rebar diameter. H is Unit Step Function. $f(x)$ in kN/mm is the force acting on per unit length along both crack faces due to rebar force, which is obtained according to the principle that the integration of $f(x)$ over the cracked domain is equal to the total rebar force F. Correspondingly, $f=F/d_b$ is the value of $f(x)$.

With the COD calculation equations derived in this section, the crack mouth opening displacements (CMODs) due to applied load, um_a, and rebar bridging force, um_b, are obtained if the virtual load P acts on the crack mouth. Thus

$$um_a=u_a(0)=\frac{4}{E'}\int_0^a\left[\int_0^{a'}G(x',a',b)\sigma\left(1-\frac{2x'}{b}\right)dx'\right]G(x,a',b)da' \quad (17)$$

$$\begin{aligned}um_b&=u_b(0)\\&=-\frac{4}{E'}\int_0^a\left[\int_0^{a'}G(x',a',b)f\left[H(x'-h)-H(x'-h-d_b)\right]dx'\right]G(x,a',b)da'\\&=-f\cdot um_{bunit}\end{aligned} \quad (18)$$

where um_{bunit} is CMOD due to unit linear rebar force.

2.2 CMOD due to bond slip

For RC structures, bond effect is the resistance to the relative movement between rebars and concrete. It is one of the fundamental structural behaviors because the bond slip relationship controls several phenomena, such as the collapse and the tension stiffening contribution in ultimate conditions, the crack width and spacing, and the deformability in service conditions. Thus, an adequate level of bond is required to ensure structural serviceability and safety. As for the influence of bond slip on rebar forces of cracked RC members, one of the most popular phenomenon illustrating this influence is the tension stiffening effect. Therefore, to accurately estimate rebar force of RC members, the bond effect should be taken into account.

The bond slip relation is very complicated because it is influenced by many factors, such as the concrete strength, rebar surface characteristics and embedment length. Many experimental and theoretical investigations have been carried out on rebar/concrete bond effect under various load conditions, such as monotonic load and cyclic load for various bond conditions. Several models are available in literatures (Achenbach *et al*. 1992; Doyle and Scala 1978; Nazmul and Matsumoto 2008a; Shima *et al*. 1987). By employing bond slip models for different loads and bond conditions, CMOD due to bond slip in the corresponding conditions can be obtained.

In this paper, the method is employed in analyzing a beam in (Nazmul and Matsumoto 2008a), where a newly cast beam was cracked under the monotonic load. Therefore, bond slip model for non-deteriorated conditions should be employed. Based on several bond tests conducted under various boundary conditions, (Maekawa *et al*. 2003) reported that the unique bond slip relation would not exist unless the strain of rebar is introduced into the relation because the strain is thought to be an indicator of damage concrete around rebars. Based on these considerations, a unique bond-slip-strain relation for non-deteriorated condition is proposed in the literature, which is expressed as

$$\frac{\tau}{f_c}=\frac{0.73\left(\ln\left(1+5s'\right)\right)^3}{1+\varepsilon\times10^5} \quad (19)$$

where In is natural logarithm, ε is the rebar strain, $s'=1000S/d_b$, τ and S are bond stress and slip at any point along rebar, respectively, f_c is concrete strength in MPa. The unit of slip (S) and rebar diameter (d_b) should be the same.

To ensure a crack under Mode I loading, a notch was set in the midspan of the RC beam in (Nazmul and Matsumoto 2008a). As a result, a major crack was formed in the midspan as shown in **Fig. 1** and long embedment condition was satisfied. For long embedment condition, the local bond slip relations can be well predicted too by the following simple equation in (Maekawa *et al*. 2003) as:

$$\tau=0.9f_c^{2/3}\left(1-e^{-40s^{0.6}}\right) \quad (20)$$

where $s=S/d_b$ is the normalized slip referred to the rebar

diameter. This model is employed in this study because the boundary condition of the model and the employed test identify with each other.

In addition, there are some general relations among bond stress, slip and rebar strain. As illustrated in **Fig. 2**, defining the point on rebar where both rebar strain and bond slip are equaling zero as the origin of z coordinate, the slip at point (z) is the integration of rebar strain from z to the origin. With the concept, the slip is defined as the displacement of the rebar at the point concerned measured relative to a fixed point in the concrete, and also the relative displacement between the rebar and concrete as for the long embedment condition. L_s is debonding length. This relation is simply expressed as

$$S(z)=\int_0^z \varepsilon(t)dt \tag{21}$$

where $\varepsilon(z)$ is rebar strain at any point and t is the dummy variable for the integration.

The local bond stress at any location along a rebar is proportional to the slope of the strain distribution curve at that point. **Fig. 3** shows the stresses acting on dz rebar element. The equilibrium equation of the rebar element is as

$$\tau\cdot\pi d_b\cdot dz=\frac{d\sigma_s}{dz}\cdot dz\cdot\frac{\pi d_b^2}{4} \tag{22}$$

thus

$$\tau=\frac{E_s\cdot d_b}{4}\frac{d\varepsilon}{dz}=\frac{E_s\cdot d_b}{4}\frac{d^2S}{dz^2} \tag{23}$$

Where E_s is the elastic modulus of rebar, $\sigma_s(z)$ is rebar stress at any point. $d\varepsilon/dz$ is the slope of strain distribution curve. The relations between rebar strain, bond stress and bond slip are shown in **Fig. 4**.

Equations 21 and 23 are valid under the following assumptions:
(1) Rebar has a linear elastic constitutive law in the longitudinal direction;
(2) For any point along the rebar in the debonding region, the concrete strain is negligible compared with the rebar strain.

Substituting Eq. 23 into Eq. 20, the differential equation of the normalized slip with respect to location is obtained.

$$\frac{E_s\cdot d_b^2}{4}\frac{d^2s}{dz^2}=0.9f_c^{2/3}\left(1-e^{-40s^{0.6}}\right) \tag{24}$$

For long enough embedment condition, the boundary conditions (**Fig. 2**) are:

$$z=L_s\Rightarrow\begin{cases}s=S_s/d_b\\ \sigma_s=f\cdot d_b/A\\ \varepsilon=\sigma_s/E_s\end{cases}\qquad z=0\Rightarrow\begin{cases}s=0\\ \sigma_s=0\\ \varepsilon=0\end{cases} \tag{25}$$

where A is rebar sectional area; L_s is the debonding length which is unknown. Obviously, Eq. 24 has no theoretical solution and should be solved numerically. The procedure of numerical solving is:

Step 1: Calculate $\varepsilon(L_s)=f\cdot d_b/E_s\cdot A$ and assume $S(L_s)=S_s$ arbitrarily;

Step 2: Substitute $S(L_s)$ into Eq. 20, $\tau(L_s)$ is obtained. For the region from $z=L_s$ to $z=L_s-\Delta L_s$, bond stress τ can be considered as equaling $\tau(L_s)$ if ΔL_s is small enough. Following Eq. 23 and the relations illustrated in **Fig. 4**,

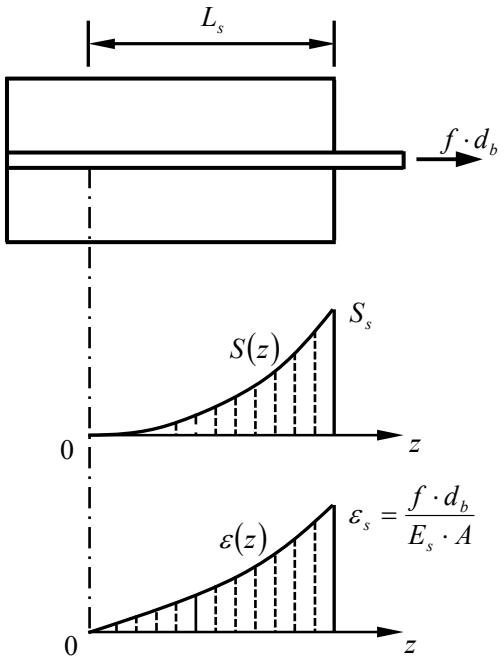

Fig. 2 Bond slip and rebar strain along rebar.

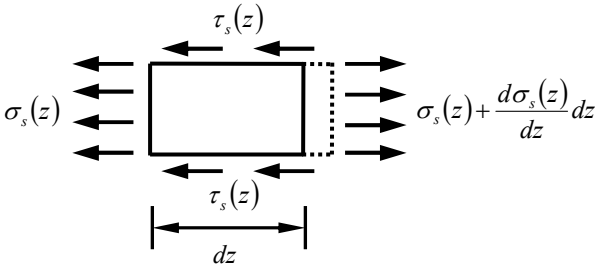

Fig. 3 Stresses acting on rebar element.

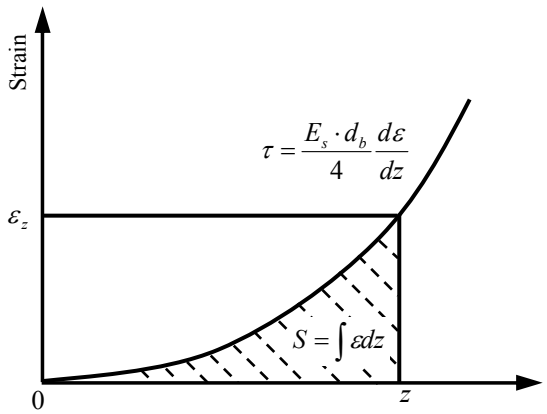

Fig. 4 Relation between rebar strain, bond stress and bond slip.

formulas for both $\varepsilon(L_s\text{-}\Delta L_s)$ and $S(L_s\text{-}\Delta L_s)$ calculations are obtained, which are expressed as:

$$\varepsilon\left(L_s-\Delta L_s\right)=\varepsilon\left(L_s\right)-\frac{\tau\left(L_s\right)}{E_s}\cdot\Delta L_s \tag{26a}$$

$$s\left(L_s-\Delta L_s\right)=s\left(L_s\right)-\frac{\varepsilon\left(L_s\right)+\varepsilon\left(L_s-\Delta L_s\right)}{2}\cdot\Delta L_s \tag{26b}$$

Step 3: Repeating Step 2, the slip and rebar strain curves are obtained. And then check whether the boundary conditions at z=0 are satisfied or not.

Step 4: Adjusting S_s and repeating Step 2 and Step 3 to ensure boundary conditions at z=0 satisfied. Consequently, the numerical result of strain to slip relation is obtained, and the debonding length L_s is obtained simultaneously.

Taking $\varepsilon(L_s)$=0.0035 as example and employing parameter values of the RC beam in (Nazmul and Matsumoto 2008a),

(1) $S(L_s)$=0.250mm is assumed;

(2) Following the Step 2, the slip and rebar strain curves corresponding to $S(L_s)$=0.250mm are obtained, which are shown in **Fig. 5**. It is found that the boundary condition, slip and rebar strain equaling zero at a same point, cannot be satisfied.

(3) Adjusting $S(L_s)$ to ensure that the boundary condition can be satisfied at a certain point. This point is the origin of z coordinate. It is found that the boundary condition is satisfied when $S(L_s)$ equals 0.278mm. The rebar strain and slip distribution curves corresponding to $S(L_s)$=0.278mm are shown in **Fig. 5** as well.

To facilitate application, the numerical result of strain to slip relation is fitted by a polynomial function. The fitting result of the strain to slip relation is simply expressed as

$$S\left(z\right)=S\left(\varepsilon\left(z\right)\right) \tag{27}$$

Both the numerical and fitting strain to slip relations are shown in **Fig. 6**.

Regarding the slip as the COD of the center point of rebars, the CMOD can be obtained by assuming the COD due to bond slip increasing linearly from rebars to the crack mouth with a slope of

$$\psi=\frac{a}{a-h-r} \tag{28}$$

where r is the rebar radius. Then the CMOD due to bond slip, $um_s(\varepsilon_s)$, is given as

$$um_s\left(\varepsilon_s\right)=S\left(\varepsilon_s\right)\cdot\psi \tag{29}$$

where $\varepsilon_s=f\cdot d_b/E_s\cdot A$ is rebar strain at crack location.

2.3 Formula for rebar force estimation

According to previous sections, the calculation formulas for CMOD due to the aforementioned three main contributions have been established. Then, the formula for rebar force estimation using CMOD is derived following the idea that the total CMOD is the summation of CMOD due to each contribution, which is expressed as

$$um=um_a+um_b+um_s=um_a-f\cdot um_{bunit}+um_s\left(\varepsilon_s\right)\cdot\psi \tag{30}$$

where um is the total CMOD. The only unknown variable for Eq. 30 is the rebar force f which can be obtained by solving the equation.

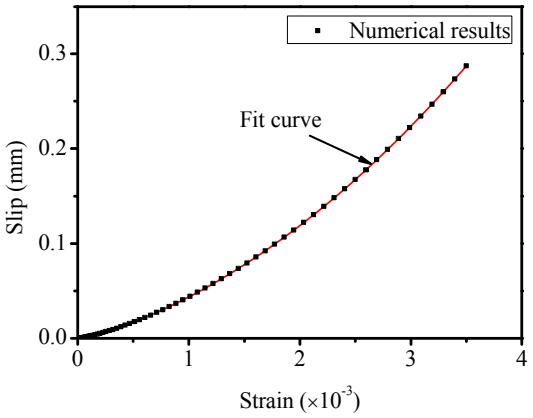

Fig. 6 Strain vs slip relation.

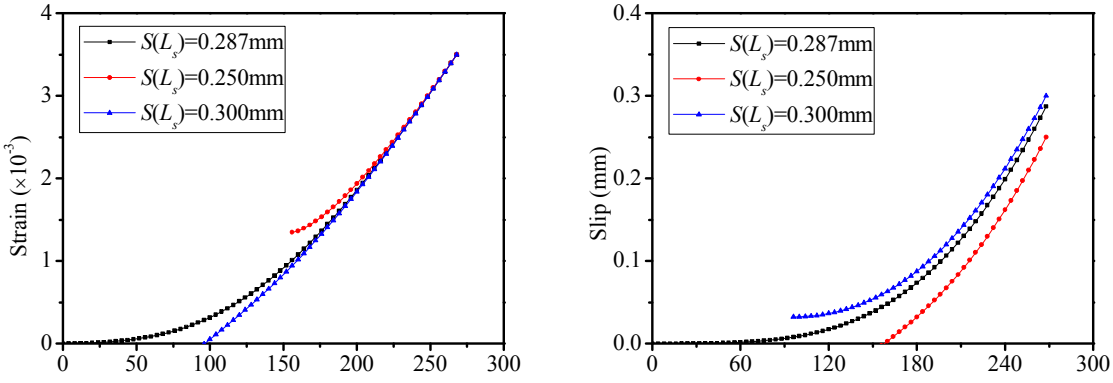

(a) Strain distribution curves (b) Slip distribution curves

Fig. 5 Strain and slip distribution curves.

Table 1 Details of the tested beam.

Parameters	Value
Concrete cylinder strength	30 MPa
Critical stress intensity factor K_{IC}	10 N/mm$^{3/2}$
Yield strength of steel	345 MPa
Young's modulus of steel	200 GPa
Young's modulus of concrete	28 GPa
Possion's ratio of concrete	0.2
Possion's ratio of steel	0.3
Beam total depth (b)	10 cm
Beam width (t)	10 cm
Clear cover (h)	32 mm
Steel rebar radius (r)	3 mm
Beam span (L)	24 cm

3. Cracked RC beam model

In this study, to facilitate the comparison with the experimental results in (Nazmul and Matsumoto 2008a), both analytical and experimental study are conducted to simulate the crack opening of the reference beam. The static crack opening experiment is briefly summarized here. The dimensions, boundary and load conditions of the specimen are shown in **Fig. 7**. To set the major crack initiation position, a notch with 3 mm width and 1 cm depth was cut at the mid-span on the bottom surface of the beam. Basic material properties and specimen dimensions are listed in **Table 1**.

4. Method inverstigation through theoretical approach

With a measuring COD profile, the rebar force can be estimated through inverse analysis of COD profile and CMOD analysis method proposed in this paper. Since the applicability and accuracy of rebar force estimation based on inverse analysis of COD profile have been accepted, the accuracy of the CMOD analysis method can be investigated by comparing the results from these two approaches in the analytical scope.

For RC beams, the sectional tension contribution of concrete is generally negligible compared with that of rebars. Neglecting the tensile strength of concrete, the rebar force is calculated based on the cracked RC beam section analysis using Eq. 15. Thus, the rebar force from Eq. 15 is on the safe side. With the rebar force from Eq. 15, the crack length, a, is determined following the criterion for crack advance in the bridged crack model under monotonic loading in the current analysis, which is

$$K_{tip} = K_a + K_b = K_{IC} \tag{31}$$

where K_a and K_b are stress intensity factors due to the external loads and the rebar forces, respectively, and K_{tip} is net stress intensity factor combining both effects, K_{IC} is the fracture toughness of reinforced concrete (see (Saouma *et al*. 1982) for details).

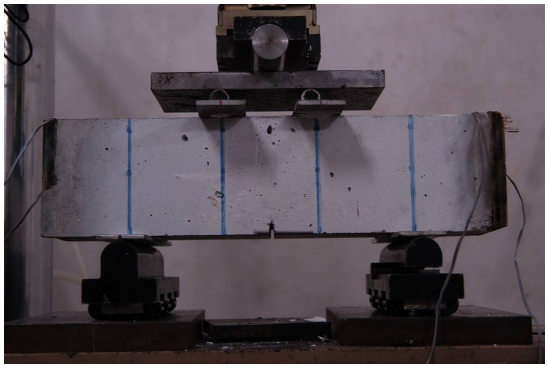

(a) Experimental set-up

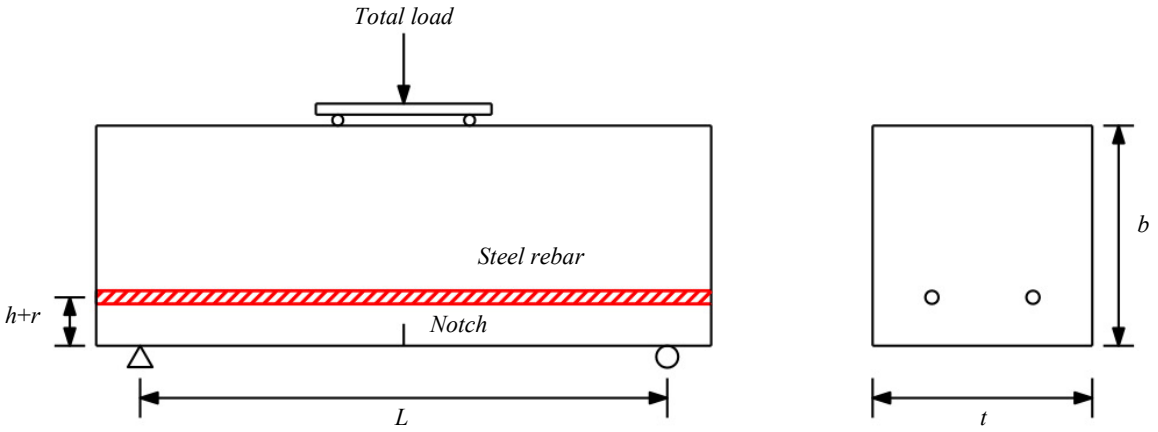

(b) Specimen details

Fig. 7 Experimental set-up and specimen details.

Then, the direct solution of Eq. 11 yields the analytical COD profiles in **Fig. 8**. Substituting the rebar force into Eq. 27, the bond slip related COD at rebar location can be obtained. Assuming a uniform bond slip related COD along the entire boundary of rebars, and assuming that this COD increases from rebars towards the crack mouth and decreases from rebars towards the crack tip with the slope determined by Eq. 28, the COD profile including slip is obtained. COD profiles naming slip included in **Fig. 8** are the summation of the direct analytical COD profiles and COD profiles due to bond slip. It is found in **Fig. 8** that, due to the existence of rebars, each analytical COD profile experiences a depression in the region of rebars, which is from the value of the horizontal axis equaling 32mm to 38mm. These depressions implicitly exhibit the influence of rebars on the local deformation. Thus, the magnitudes of the depressions depend on the rebar bridging force and rebar to concrete interface bond slip. However, this local deformation cannot be reflected on the CMOD. Only the influence of rebar bridging force and rebar to concrete bond slip on CMOD can be captured. Therefore, the CMOD due to bond slip should be

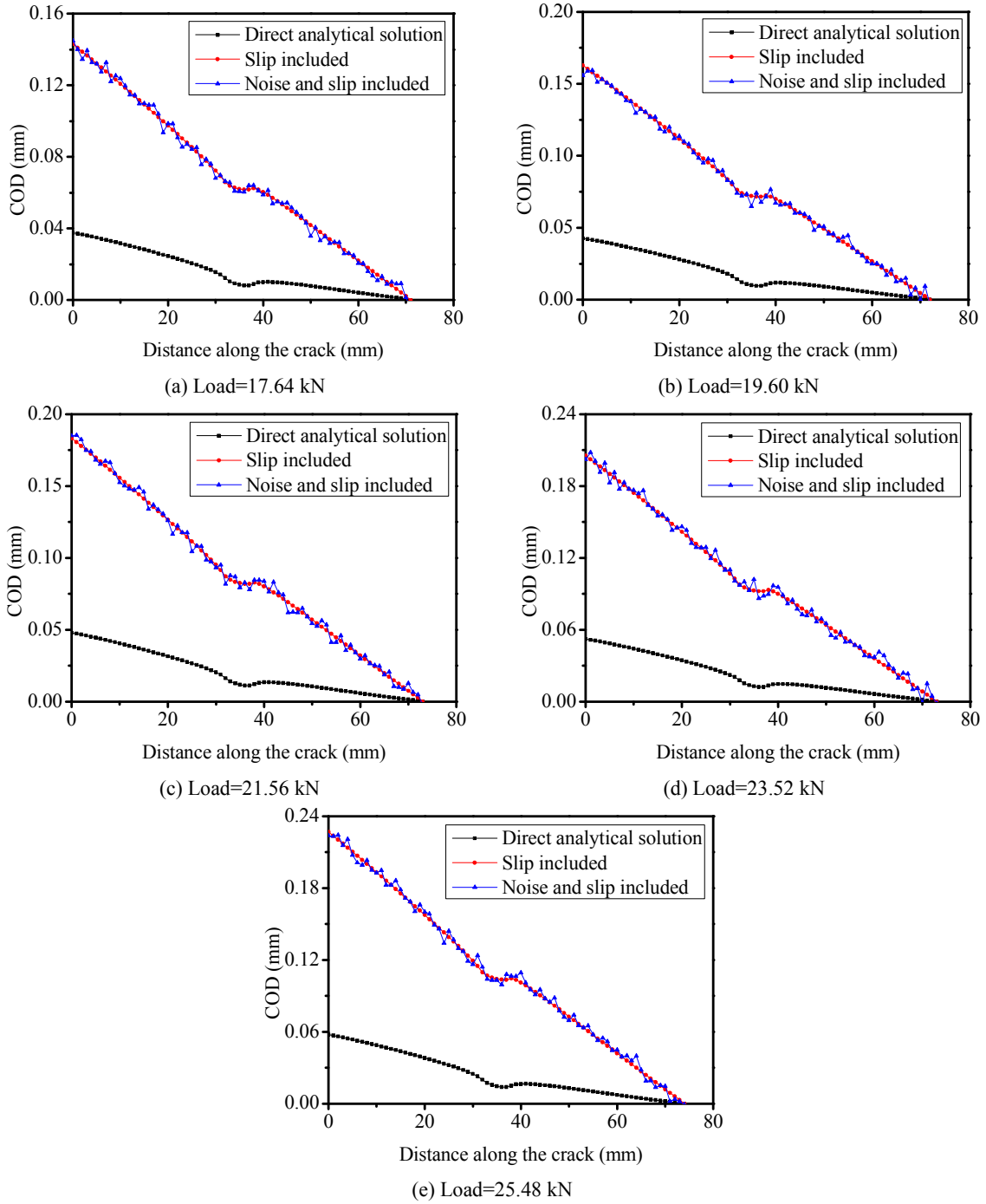

Fig. 8 Analytical COD profiles of an RC beam under static loads.

Table 2 Estimating results of inverse analysis of COD profile.

k(%)	Rebar force (N/mm^2)					Estimating error (%)				
	17.64kN	19.60kN	21.56kN	23.52kN	25.48kN	17.64kN	19.60kN	21.56kN	23.52kN	25.48kN
0.0	217.919	242.075	266.232	290.388	314.544	0.00	0.00	0.00	0.00	0.00
0.5	228.617	237.229	257.468	298.728	321.081	-4.679	1.968	3.004	-2.792	-2.036
1.0	207.784	229.710	290.832	276.431	288.248	4.878	5.383	-8.458	5.049	9.123
1.5	260.498	266.544	307.794	307.108	359.565	-16.345	-9.180	-13.503	-5.444	-12.521
2.0	191.264	348.145	356.196	351.377	367.796	13.936	-30.467	-25.257	-17.357	-14.479

Table 3 Estimating results of CMOD analysis.

k(%)	Rebar force (N/mm^2)					Estimating error (%)				
	17.64kN	19.60kN	21.56kN	23.52kN	25.48kN	17.64kN	19.60kN	21.56kN	23.52kN	25.48kN
0.0	217.919	242.075	266.232	290.388	314.544	0.00	0.00	0.00	0.00	0.00
0.5	212.550	237.232	262.238	283.135	311.329	2.526	2.042	1.523	2.561	1.032
1.0	209.665	240.020	260.760	284.606	309.030	3.937	0.856	2.098	2.031	1.784
1.5	216.229	237.557	261.623	288.159	309.780	0.782	1.902	1.761	0.773	1.538
2.0	210.403	243.894	259.406	281.862	312.641	3.572	-0.746	2.631	3.025	0.609

considered separately by exploiting a bond slip model. This is the mainly difference between inverse analysis of COD profile and the CMOD analysis method. It can be also found that the COD due to bond slip takes up a great proportion of the total COD in all cases, even before steel yielding, which means the CMOD due to bond slip is not negligible.

In reality, the COD profile collected either from laboratory or field experiment contains noise inevitably due to instrumental error and human oversight. In this study, the noise is simulated by random numbers of Gaussian distribution with zero mean and a certain standard of deviation (ω). Thus, ω is the only criterion for noisy level. The deviation of inputting noise is calculated as

$$\omega = k \cdot \max[u] \tag{32}$$

where u is the analytical crack mouth opening displacements; k is a dimensionless coefficient.

The inputted noise may cause many unexpected fluctuations on the COD profile, and the amplitudes of the fluctuations increase with the increasing noise content in noisy COD profile. The noisy COD profiles with k equaling 2% are shown in **Fig. 8**. It is found that the noise can stir up fluctuations of similar amplitudes with that of the depression due to the presence of rebars. This similarity leads to the results of inverse analysis of COD profile being unreliable, even though the rebar force estimation error using the noisy COD profiles may be small by coincidence owing to the randomness of noise. Therefore, only noisy COD profiles with k less than or equal to 2% are employed in analysis.

With the synthetic noisy COD profiles, rebar forces corresponding to COD profiles with different levels of noise can be estimated based on the inverse analysis of COD profile method in (Nazmul and Matsumoto 2008a) and the CMOD analysis model proposed in this study, which are shown in **Table 2** and **Table 3**, respectively. Since the rebar force from Eq. 15 is employed in determining the crack depth based on Eq. 31 and calculating the theoretical COD profile, the rebar force calculated by using Eq. 15 is regarded as theoretical rebar force. The errors in rebar force estimation in **Table 2** and **Table 3** are calculated by

$$\text{Estimating error (\%)} = \frac{\text{Theoretical result - Estimating result}}{\text{Theoretical result}} \tag{33}$$

It can be seen from **Table 2** and **Table 3** that excellent accuracy is achieved for both methods if the COD data is noiseless. The rebar forces are estimated with good accuracy within moderate levels of noise. The accuracy decreases with increasing error percentages of COD data.

For almost all cases, the CMOD analysis model has better accuracies than the inverse analysis of COD profile and loses accuracy at a lower speed. This can be explained as: assuming the bridging forces as a continuous function $p(x)$, then the COD, $u(x)$, is given by

$$u(x) = \frac{4}{E'}\int_x^a \left[\int_0^{a'} G(x',a',b)\left[\sigma(x') - p(x')\right]dx'\right] G(x,a',b)\,da' \tag{34}$$

For a crack on a structure under applied loads, a and $G(x, a, b)$ are invariable. Thus

$$u(x) \propto \int_x^a \int_0^{a'} p(x')\,dx'da' \tag{35}$$

and

$$p(x) \propto \frac{d^2u(x)}{dx^2} \tag{36}$$

which means the bridging force, $p(x)$, is proportional to the curvature of the COD profile, $u(x)$. Therefore, the error of the inverse analysis of COD profile is mainly relevant to the ratio of the fluctuation amplitude caused by noise to the depression due to rebars, while the error for the CMOD analysis method is proportional to the ratio of fluctuation amplitude of noise to the total CMOD. As a result, the accuracy of the CMOD analysis model is more stable than the inverse analysis of COD profile.

Table 4 CMOD under different loads.

Load (kN)	15.68	17.64	19.60	21.56	23.52	25.48
$CMOD_{max}$ (mm)	0.106	0.125	0.144	0.181	0.201	0.228
$CMOD_{ext}$ (mm)	0.112	0.132	0.156	0.192	0.221	0.257

Table 5 Comparison of results from different approaches.

Load (kN)	Rebar force (N/mm^2)				Estimating error (%)		
	(1) Inverse analysis of COD profile	(2) Analysis of COD_{max}	(3) Analysis of COD_{ext}	(4) Section analysis	[(4)-(1)]/(4)	[(4)-(2)]/(4)	[(4)-(3)]/(4)
15.68	311.090	No solution	No solution	193.763	-60.55	No solution	No solution
17.64	304.202	257.861	244.565	217.919	-39.59	-18.33	-12.23
19.60	257.835	311.024	278.383	242.075	-6.51	-28.48	-15.00
21.56	318.32	286.786	265.069	266.232	-19.56	-7.72	0.44
23.52	300.75	318.368	278.009	290.380	-3.57	-9.64	4.26
25.48	319.266	322.781	287.311	314.544	-1.48	-2.62	8.66

5. Method application

The crack width and depth data at different load levels were collected by a laboratory apparatus consisting of a microscopic digital camera and a three-axis controlled system as described in (Nazmul and Matsumoto 2008a). Since the focus of this study is a Mode I fracture problem, a notch was set at the mid-span on the bottom face of the beam to ensure the major crack initiates from this position. As a result, under four-point bending load, the major crack of the RC beam will propagate vertically and almost no shear forces will be transferred across the crack because the crack remains confined in the pure bending region all the time.

The COD data were collected at points with 1 mm spacing along the crack. The experimental COD profiles are drawn by collecting the isolated COD data points with straight line as shown in **Fig. 9**. Random fluctuations are observed, which is due to both inherent toughness of the fracture surface, such as aggregates, impurities and voids, and errors in COD measurement.

In this study, firstly, the maximum COD, COD_{max}, is treated as the experimental CMOD for rebar force estimation. This treatment seems to be more reasonable when considering the adopted assumption that is the tensile stresses in the concrete are negligible comparing with that of rebars.

However, due to the existence of the notch, the COD_{max} should be still smaller than the actual experimental CMOD. Thus, another experimental CMOD indicated as COD_{ext} is employed for rebar force estimation as well. The COD_{ext} is determined by extending the COD profile to the bottom surface of the beams following the linear polynomial fitting function of the experimental COD profile. The reasons for using the linear polynomial function are, firstly, to reduce the influence of the fitting curve slope in the immediate vicinity of the notch, because the slope is determined by the COD data closing to the notch; secondly, a strong linear relation is observed in crack faces for all conditions, which is basically abide to a generally accepted assumption for RC beam behavior under bending, plane cross-section assumption. The fitting curves and functions for the experimental COD profiles are shown in **Fig. 9**. Both of these two kinds of CMOD are listed in **Table 4**.

Table 5 shows the rebar force estimation results from different approaches: (1) Inverse analysis of COD profile by employing Tikhonov regularization method in (Nazmul and Matsumoto 2008a); (2) CMOD analysis method using COD_{max}; (3) CMOD analysis method using COD_{ext}; (4) Standard RC cracked beam transformed section analysis as stated in Eq. 15, which is regarded as theoretical rebar force because for RC beams the sectional tension contribution of concrete is generally considered as negligible compared with that of rebar. Comparing with results from approach (4), the estimating errors of each method can be obtained, which are listed in **Table 5** as well.

It is found that the accuracy of CMOD analysis method, especially using COD_{ext}, is generally higher than the inverse analysis of COD profile, whereas the accuracy difference between these two methods is not as obvious as that shown in analytical approach. The reason is: for CMOD analysis method, in analytical study, the only source of error is the noise simulating measurement error, while, in experimental study, the local bond slip model employed contains error as well; for inverse analysis method of COD profile, the actual bond slip is included implicitly.

For a load level equal to 15.68 kN, the estimating error for inverse analysis of COD profile is very high and Eq.(30) has no solution for using either COD_{max} or COD_{ext}. This is caused by the errors in the experimental COD profile where random fluctuations are observed, especially at the region close to the crack mouth.

Assuming

$$g(f) = um - um_a + f \cdot um_{bunit} - um_s(\varepsilon_s) \cdot \psi \tag{37}$$

The differential equation of Eq.(37) with respect to f is

$$\frac{dg(f)}{df} = um_{bunit} - \frac{d_b}{E_s \cdot A} \cdot \left.\frac{dum_s}{d\varepsilon}\right|_{\varepsilon=\varepsilon_s} \cdot \psi \tag{38}$$

For load equaling 15.68 kN, um_{bunit}=6.39×10^{-5} *mm*. According to **Fig. 1**, $dum_s/d\varepsilon \in$ {80mm, 110mm}, then

the second term in the left part of Eq. 38 should belong to $\{8.9\times10^{-5}$ mm, 1.2×10^{-4} mm$\}$. As a result

$$\frac{dg(f)}{df} < 0 \tag{39}$$

while $g(0) < 0$. Thus, Eq. 30 has no solution.

6. Sensitivity study

This study aims at developing a maintenance technique for existing structures based on field measurement data. The reliability and anti-interference ability deserve great attention. Since the result error is mainly from the measurement error of CMOD according to previous analysis, result sensitivity study on error in CMOD was also carried out.

In theoretical scale, the CMOD, the left term of Eq. 30, can be calculated through direct analysis. By inputting different levels of error into it and solving Eq. 30, the corresponding rebar force error vs CMOD error relation can be obtained, as shown in Fig. 10. The errors of

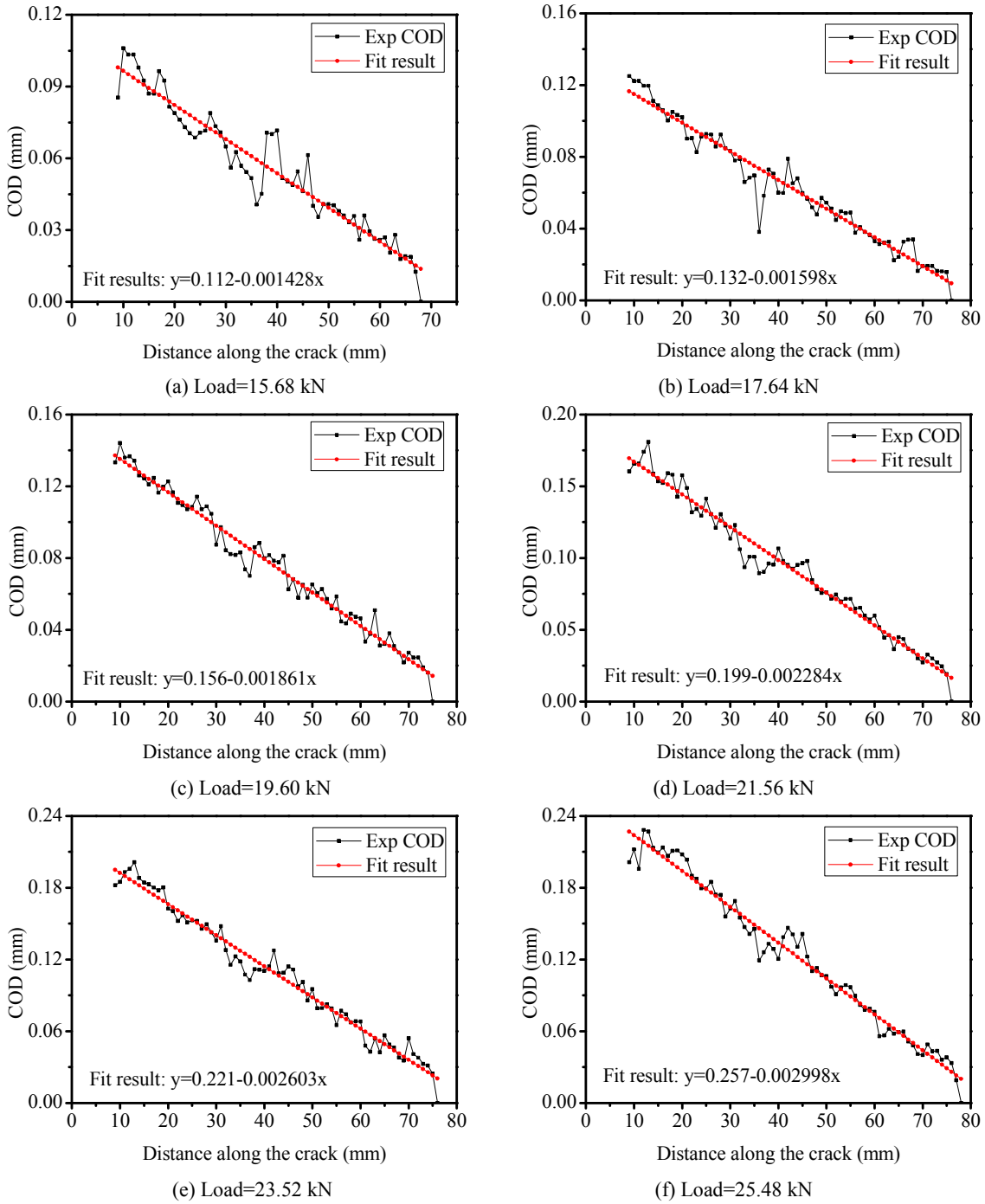

Fig. 9 Experiment COD profiles of an RC beam under static loads.

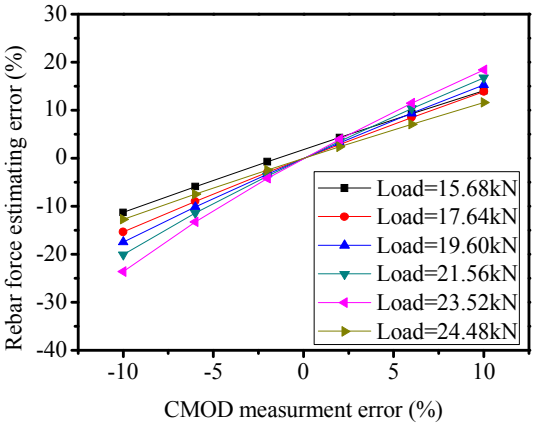

Fig. 10 Sensitivity study of CMOD measurement error.

CMOD and rebar force are defined as Eq. 40.

$$\text{PRM error}\ (\%) = \frac{\text{PRM with- PRM without error}}{\text{PRM without error}} \times 100 \quad (40)$$

where PRM is the abbreviation of parameter. It is found that the accuracy loses with the increasing of noise level almost linearly. This can be explained by Eq. 37. The positive slope means the estimated rebar force increases with the decrease of CMOD which really makes sense because larger rebar force lead to smaller crack opening and can be explained by Eq. 37 as well.

7. Conclusions

Following the mechanisms of concrete cracking for RC structures, the relation between crack mouth opening displacement (CMOD) and the rebar forces crossing a crack under model I loading is developed based on fracture mechanics and bond slip model. Correspondingly, a rebar force estimation method through CMOD analysis is established. As the CMOD due to bond slip is calculated by employing a bond slip model, the tensile stiffness effect which illustrates the influence of bond slip on the rebar forces in cracked RC members is taken into account. Similarly, the rebar force for an RC structure maybe estimated if the bond slip model corresponding to the bond slip condition of the structure is employed.

Theoretically, with the same noisy synthetic COD profile, rebar forces are estimated by the proposed CMOD analysis method and the inverse analysis method of COD profile. For the cracked RC beam in (Nazmul and Matsumoto 2008a), the applicability and stability of the proposed CMOD analysis method are verified by the smaller rebar force estimation error compared with the error from the inverse analysis method of COD profile. Findings show that bond slip of deformed bar is an important contribution of crack opening even before steel yielding occurs, which means the estimated rebar force using the tested CMOD should be much smaller than the actual rebar force if the CMOD due to bond slip is not included.

The proposed CMOD analysis method is then employed successfully in rebar force estimation for a RC beam cracked under four-point bending tests. Since the error for CMOD analysis method is proportional to the ratio of fluctuation amplitude due to noise to the experimental CMOD while the error of inverse analysis of COD profile is mainly relevant to the ratio of the fluctuation amplitude due to noise to the depression due to rebars, better accuracy and stability of rebar force estimation are observed for CMOD analysis method than the inverse analysis of COD profile. This further verifies the applicability and stability of the proposed method.

Since the accuracy of rebar force estimation depends on the accuracy of CMOD measurement and the employed bond slip model, more sophisticated techniques of CMOD measurement, such as treating the average value of CMODs on the bottom face of the beams as the experimental CMOD, should be adopted. Considering the primary error source is measurement CMOD, sensitivity study has been conducted on it. It is found that the errors of rebar force estimation increased almost linearly with the amount of error inputted into the CMOD. This result further emphasized the importance of improving the accuracy of obtaining it.

The most important advantage of this method lies in the fact with CMOD and crack depth, the imbedded rebar force for existing RC structures can be estimated. For CMOD, it is easily measurable. In terms of crack depth, for many kinds of cracks such as 3D cracks and cracks with complex configurations, the crack depth has been successfully measured using ultrasonic techniques (Chang and Wang 1997; Seher *et al*. 2013). Therefore, this method provides a potential non-destructive test and evaluation (NDT & E) approach for structure health monitoring of existing RC structures where the COD profile is unmeasurable.

References

Achenbach, J. D., Komsky, I. N., Lee, Y. C. and Angel, Y. C., (1992). "Self-calibrating ultrasonic technique for crack depth measurement." *J. Nondestruct. Eval.*, 11(2), 103-108.

Ben Romdhane, M. R. and Ulm, F. J., (2002). "Computational mechanics of the steel–concrete interface." *Int. J. Numer. Meth. Eng.*, 26(2), 99-120.

Buchanan, D. J., John, R. and Johnson, D. A., (1997). "Determination of crack bridging stresses from crack opening displacement profiles." *Int. J. Fracture*, 87(2), 101-117.

Bueckner, H. F., (1970). "Novel principle for the computation of stress intensity factors." *Zeitschrift fuer Angewandte Mathematik & Mechanik.,* 50(9), 529-546.

Chang, Y.-F. and Wang, C.-Y., (1997). "A 3-D image detection method of a surface opening crack in concrete using ultrasonic transducer arrays". *J. Nondestruct. Eval.*, 16(4), 193-203.

Cox, B. N. and Marshall, D. B (1991). "The

determination of crack bridging forces." *Int. J. Fracture*, 49(3), 159-176.

Cox, B. N. and Marshall, D. B., (1991). "Stable and unstable solutions for bridged cracks in various specimens." *Acta metallurgica et materialia*, 39(4), 579-589.

Doyle, P. A. and Scala, C. M., (1978). "Crack depth measurement by ultrasonics: a review." *Ultrasonics*., 16(4), 164-170.

Eligehausen, R., Popov, E. P. and Bertero, V. V., (1982). "Local bond stress-slip relationships of deformed bars under generalized excitations." In: *Proc., 7th Euro. Conf. on Earthquake Eng*., *Athens: Techn*, Vol. 4, Chamber of Greece, 68-80.

Fett, T., Munz, D., Seidel, J., Stech, M. and Rödel, J., (1996). "Correlation between long and short crack R-curves in alumina using the crack opening displacement and fracture mechanical weight function approach." *J. Am. Ceram. Soc.*, 79(5), 1189-1196.

Harajli, M., Hamad, B. and Karam, K., (2002). "Bond-slip response of reinforcing bars embedded in plain and fiber concrete." *J. Mater. Civil. Eng*., 14(6), 503-511.

Li, V. C. and Liang, E., (1986). "Fracture processes in concrete and fiber reinforced cementitious composites." *J. Eng. Mech.*, 112(6), 566-586.

Li, V. C. and Matsumoto, T., (1998). "Fatigue crack growth analysis of fiber reinforced concrete with effect of interfacial bond degradation." *Cement Concrete Comp.*, 20(5), 339-351.

Maekawa, K., Pimanmas, A. and Okamura, H. A., (2003). "*Non-linear mechanics of reinforced concrete*." CRC Press, London and New York.

Marshall, D. B., Cox, B. N. and Evans, A. G., (1985). "The mechanics of matrix cracking in brittle-matrix fiber composites." *Acta metallurgica*., 33(11), 2013-2021.

Marshall, D. B. and Cox, B. N., (1987). "Tensile fracture of brittle matrix composites: influence of fiber strength." *Acta metallurgica.*, 35(11), 2607-2619.

McMeeking, R. M. and Evans, A. G., (1990). "Matrix fatigue cracking in fiber composites." *Mech. Mater*, 9(3), 217-227.

Nazmul, I. M. and Matsumoto, T., (2003). "Determination of steel stresses in reinforced concrete structures from crack opening profile." *Proceedings of the Structural Health Monitoring and Intelligent Infrastructure*, 739-746.

Nazmul, I. M. and Matsumoto, T., (2008a). "High resolution COD image analysis for health monitoring of reinforced concrete structures through inverse analysis." *Int. J. Solids Struct.*, 45(1), 159-174.

Nazmul, I. M. and Matsumoto, T., (2008b). "Regularization of inverse problems in reinforced concrete fracture." *J. Eng. Mech.*, 134(10), 811-819.

Okamura, H., Maekawa, K. and Sivasubramaniyam, S., (1985). "Verification of modeling for reinforced concrete finite element." Paper presented at the *Finite element analysis of reinforced concrete structures*.

Rice, J. R., (1972). "Some remarks on elastic crack-tip stress fields." *Int. J. Solids Struct.*, 8(6), 751-758.

Salem, H. M. and Maekawa, K., (2004). "Pre-and postyield finite element method simulation of bond of ribbed reinforcing bars." *J. Struct. Eng.*, 130(4), 671-680.

Saouma, V., Ingraffea, A. and Catalano, D., (1982). "Fracture Toughness of Concrete: K I c Revisited." *Journal of the Engineering Mechanics Division*, 108(6), 1152-1166.

Seher, M., In, C.-W., Kim, J.-Y., Kurtis, K. E. and Jacobs, L. J., (2013). "Numerical and experimental study of crack depth measurement in concrete using diffuse ultrasound." *J. Nondestruct. Eval*., 32(1), 81-92.

Shima, H., Chou, L.-L. and Okamura, H., (1987). "Micro and macro models for bond in reinforced concrete." *J. Fac. Eng. Archit. Gaz*., 39(2), 133-194.

Sokolnikoff, I. S. and Specht, R. D., (1956). "*Mathematical theory of elasticity*." McGraw-Hill, New York.

Tada, H., Paris, P. G. and Irwin, G. R., (2000). "*The analysis of cracks handbook*." ASME Press , New York.